Journal of Alloys and Compounds 509 (2011) 8183–8188

Contents lists available at ScienceDirect

Journal of Alloys and Compounds

journal homepage: www.elsevier.com/locate/jallcom

Two step novel chemical synthesis of polypyrrole nanoplates for supercapacitor application

D.P. Dubal, S.V. Patil, A.D. Jagadale, C.D. Lokhande*

Thin Film Physics Laboratory, Department of Physics, Shivaji University, Kolhapur 416004 (M.S), India

ARTICLE INFO

Article history:
Received 9 February 2011
Received in revised form 8 March 2011
Accepted 13 March 2011
Available online 21 March 2011

Keywords:
Polypyrrole nanoplates
SEM
TEM
Supercapacitor
Charge–discharge

ABSTRACT

Simple and inexpensive two step novel chemical method for the synthesis of polypyrrole (PPy) nanoplates has been reported. These PPy nanoplates are characterized with X-ray diffraction (XRD), Fourier transform infrared (FTIR) spectroscopy, scanning electron microscopy (SEM) and transmission electron microscopy (TEM). Polypyrrole nanoplates exhibit amorphous nature as confirmed from XRD study. Based on SEM and TEM analysis, the formation of the spherical bunches of PPy nanoplates with average size of about 20 nm are inferred. The electrochemical performance of PPy electrode was evaluated by cyclic voltammetry (CV) and galvanostatic charge–discharge measurement. A high specific capacitance of 533 F g^{-1} was obtained within the potential range of −0.4 to 0.6 V in 0.5 M H_2SO_4 solution. Moreover, PPy electrode exhibited high discharge/charge efficiency of 93% and the capacitance retention of 83% at a current density of 10 mA cm^{-2} indicating good electrochemical reversibility and rate capability.

1. Introduction

Growing demands for the generation of power sources with transient high-power density have stimulated great interest in electrochemical capacitors in recent years. Supercapacitors are designed to bridge the gap between batteries and capacitors to form fast charging energy-storage devices of intermediate specific energy. They are seen to have a potential market both in hybrid electric vehicles and pure electric vehicles to improve regenerative braking (through fast charge capability) and deliver larger acceleration (through fast discharge capability). On the basis of electrode materials used and the charge storage mechanisms, supercapacitors can be classified into: (a) electric double layer capacitors which employ carbon or other materials with large surface area as electrodes and (b) redox supercapacitors in which electroactive materials such as transition metal oxides or conducting polymers are applied as electrodes [1–3]. Conducting electroactive polymers remain a subject of intense investigation of many research groups worldwide. The conducting polymers have electrochemical characteristics of rapidly reversible doping and dedoping ability so that they can store the charge throughout the entire volume. Among several kinds of conducting polymers for the supercapacitor, such as polypyrrole (PPy), polyaniline (PANI), poly (3-methylthiopine) (PMET), poly (1,5-diaminoanthraquinon)(PDAAQ), poly (3,4-ethylenedioxythiopene) (PEDOT), PPy is an intrinsically conducting polymer because of its high conductivity, high storage ability, good thermal and environmental stability, high redox and capacitive current and biocompatibility [4–6].

The electrochemical properties of PPy based electrodes depend on the electrodes preparation methods and also the effective surface area of the electrodes. So far, research groups worldwide have mainly focused on modification of PPy based materials, such as optimizing the conditions of PPy preparation including current density, pH value, temperature, concentration of pyrrole (Py) monomer, types and concentrations of doping ions [7], and preparing PPy based composite films to achieve larger effective surface area by nanotechnology [8,9]. But there is much less attention on increasing the specific capacitance of supercapacitor (or electrode of supercapacitor) by structuring the substrate of the supercapacitor with large effective surface area for PPy electrodes deposition.

Yang et al. [10] prepared coaxial halloysite/polypyrrole tubular nanocomposites by the in situ chemical oxidative polymerization method and reported a maximum supercapacitance of 522 F g^{-1} in 0.5 M Na_2SO_4 electrolyte. An et al. [11] reported a supercapacitance of 433 F g^{-1} for polypyrrole/carbon composite prepared by chemical oxidation polymerization through ultrasound irradiation. Shi et al. [12] prepared polypyrrole films by anodic electropolymerization on stainless steel substrates from aqueous pyrrole solutions containing sodium salicylate and tiron additives and reported supercapacitance of 254 F g^{-1} in 0.5 M Na_2SO_4 electrolyte. Thus, the performance electrochemical supercapacitor of polypyrrole may be influenced by the morphology, which is closely related to the preparation methods and conditions.

* Corresponding author. Tel.: +91 231 2609229; fax: +91 231 2692333.
E-mail address: l.chandrakant@yahoo.com (C.D. Lokhande).

0925-8388/$ – see front matter © 2011 Elsevier B.V. All rights reserved.
doi:10.1016/j.jallcom.2011.03.080

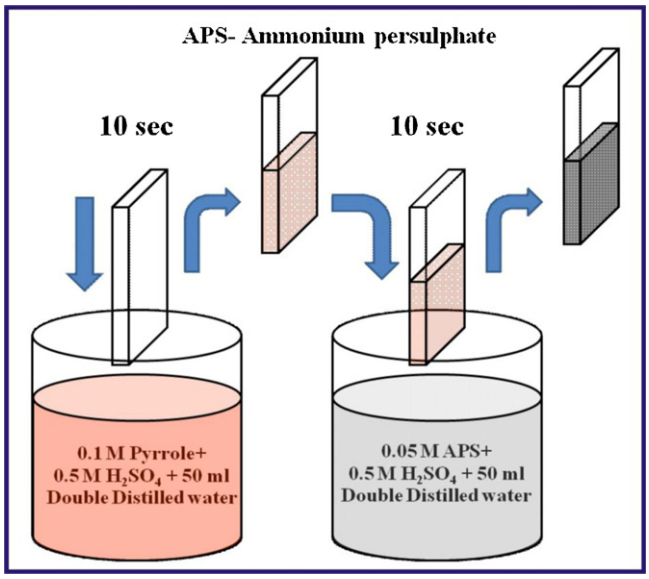

Fig. 1. The schematic representation of two step chemical method for synthesis of PPy thin films.

The cost effectiveness and ease of synthesis are the important factors in the successful commercialization of high conductivity. In this work, we fabricate 3D spherical bunches of PPy nanoplates with large effective surface area for supercapacitor by employing simple and inexpensive two step chemical route. The key steps in our developed process flow include two step chemical polymerization of PPy, characterization of these PPy electrodes by XRD, FTIR, SEM and TEM techniques. Then the electrochemical behaviors of the PPy electrodes were investigated by electrochemical tests.

2. Experimental details

Two beakers system is used for the deposition of polypyrrole (PPy) thin films onto stainless steel substrates. First beaker contains the solution of 0.1 M pyrrole prepared in 1 M H_2SO_4 and double distilled water; serve as cationic precursor at room temperature. Second beaker contains 0.05 M solution of ammonium persulphate in 1 M H_2SO_4 and double distilled water at room temperature acts as oxidizing agent and hydrogeno sulphate anions from the decomposition of ammonium persulphate participate as anion precursor. The well cleaned stainless steel substrates were dipped in cationic precursor i.e. acidic pyrrole solution for 10 s in which pyrrole monomers are adsorbed onto substrate surface. After immersion of the substrate into the ammonium persulphate solution for 10 s, the reaction occurred at substrate surface to form blackish polypyrrole polymer. Thus one cycle of polypyrrole deposition is completed. This cycle was repeated several times to increase the thickness of polypyrrole film. The schematic representation of two step chemical method is shown in Figs. 1 and 2.

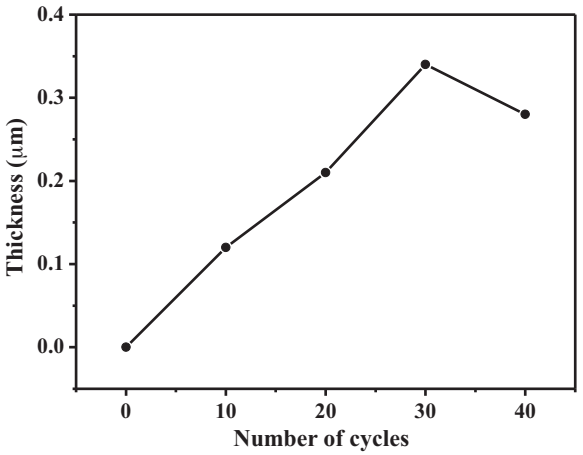

Fig. 2. Variation of PPy film thickness with deposition cycles.

The mass of PPy films were determined using the electronic microbalance (Tapson's 100TS). The structural characterization of films were studied by using Philips PW-1710 X-ray diffractometer with Cr-Kα radiation (λ = 2.2896 Å). The Fourier transform infrared (FTIR) spectra of the samples were collected using a 'Perkin Elmer, FTIR Spectrum one' unit. The morphologies of the PPy films were examined by a field emission scanning electron microscope (JEOL JSM-6360). Electrochemical studies were performed using a standard three-electrode cell containing a 0.5 M H_2SO_4 aqueous solution. The counter electrode was platinum gauze, and the reference electrode was a saturated calomel electrode (SCE). Charge–discharge and impedance study were carried out using CHI 660D electrochemical workstation.

3. Results and discussion

3.1. Reaction mechanism

Chemical polymerization is a simple and fast process with no need for special instruments. During the chemical polymerization of pyrrole, electroneutrality of the polymer matrix is maintained by incorporation of anions from the reaction solution. These counterions are usually the anions of the chemical oxidant or reduced product of oxidant. In present investigation ammonium persulphate (APS) is used as chemical oxidant for chemical polymerization. The possible reaction mechanism for chemical polymerization of PPy is given as follows [13]:

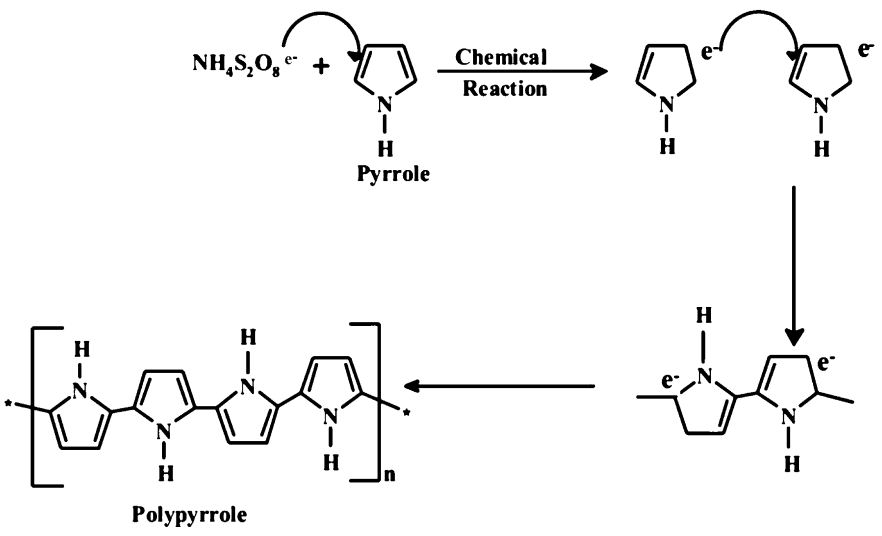

As the substrate is immersed in the first beaker the pyrrole monomer is adsorbed on the substrate due to electrostatic force of attraction. Further the substrate immersed in the second beaker then the free electrons in APS was combined with one of the pyrrole electron by breaking the pi bond in the pyrrole. The free electron in pyrrole attacks on another pi bond of another pyrrole to form a pair by creating a free electron and growth of polypyrrole takes place.

3.2. Thickness measurement

Film thickness is important parameter in the study of film properties. One of the most convenient and earliest method i.e. gravimetric weight difference method was used for determining thickness of PPy film. In this method, area and weight of the film are measured. The thickness was calculated [14].

$$T = \frac{M}{\rho A} \quad (1)$$

$$M = m_2 - m_1 \quad (2)$$

where T is film thickness, M is mass of the film material (in g), A is area of the film (cm^2), m_1 is mass of the substrate without film, m_2 is mass of the substrate with film and ρ is density of the film material (polypyrrole = 1.5 gm/cm^3). The maximum thickness obtained for PPy thin film was 0.34 μm and used for the further characterization.

3.3. Structural and FTIR studies

The X-ray diffraction pattern of polypyrrole nanoplates is depicted in Fig. 3. The peaks marked by triangle are due to the stainless steel substrate. Fig. 3 declares the absence of any sharp diffraction line, indicating that the deposited polypyrrole film is amorphous, similar to the results reported elsewhere [15] for polypyrrole films deposited by greener mechanochemical route.

Fig. 4 shows the FTIR spectrum in transmission mode of polypyrrole film deposited on stainless steel substrate. The band observed at 3412 cm^{-1} assigned to –OH vibration band corresponding to water. The transmission peak of polypyrrole at 2928 and 2853 cm^{-1} corresponds to N–H characteristic bond present in aromatic amines. The absorption band at 1554 cm^{-1} is assigned to the pyrrole ring, i.e. the combination of C=C and C–C stretching vibrations. The band at1457 cm^{-1} is associated with the C–N stretching vibration [16]. Furthermore, the bands at 1045 and 1300 cm^{-1} can be ascribed to C–H deformation vibrations and C–N stretching vibrations, respectively [17]. In addition, the C–N stretching vibrations were found at around 1177 cm^{-1} [17]. The band at 916 cm^{-1} is assigned to C=C in-plane bending of pyrrole ring [18]. Here

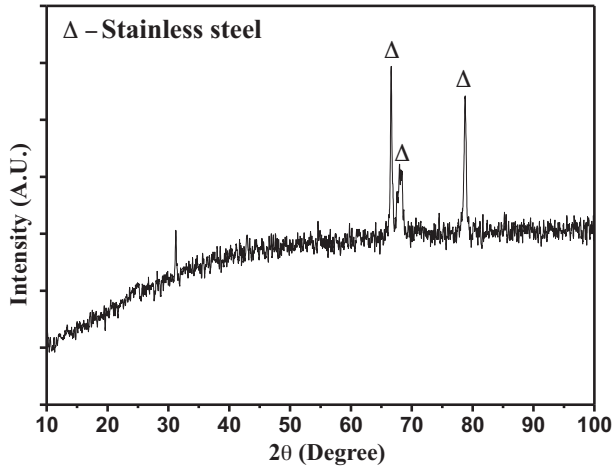

Fig. 3. The XRD pattern of PPy thin films deposited on stainless steel substrate.

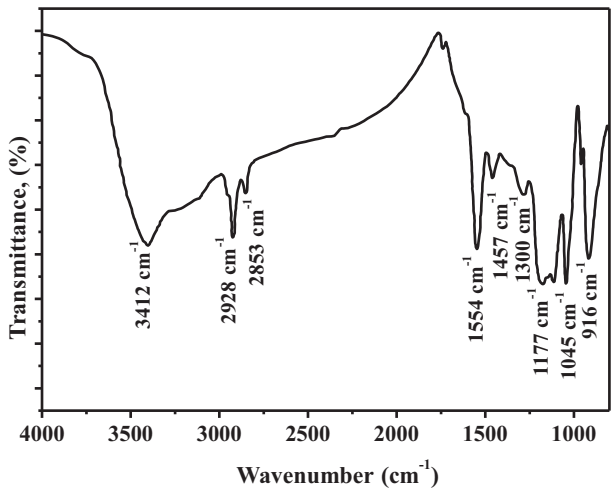

Fig. 4. The FTIR spectrum of PPy thin film.

1177 cm^{-1} and 916 cm^{-1} indicate the doping state of PPy [19]. These characteristic bands confirmed the formation of conducting polypyrrole thin films.

3.4. SEM and TEM studies

The two-dimensional surface morphology of the PPy thin films has been studied using FESEM images. Fig. 5(a) and (b) shows the FESEM images of PPy thin film at different magnifications. Formation of 3D architecture of PPy surface with coalesced nanoplates is clearly seen from SEM images. The low magnification (Fig. 5a) image confirms the formation of spherical bunches of interconnected PPy nanoplates. These nanoplates are relatively smooth and randomly distributed over the substrate. High magnified image (Fig. 5b) gives a description that these nanoplates are with approximately average size in the range 20–50 nm. The micrograph shows the agglomeration of interconnected nanoplates. The contrast in the FESEM image (Fig. 5a) shows that the film has hollow cavities which are highly porous. The porous nature of the PPy makes it a potential candidate for various surface related applications.

The morphology consisting strongly interconnected plates was further studied with high magnified TEM analysis as shown in Fig. 5(c). It shows that the film composed of interconnected nanoplates of average diameter around 30 nm, which is in consistent with plates size calculated from FESEM studies.

3.5. Wettability study

An empirical diagnostic method for evaluation of wetting property of film is the measurement of water contact angle (θ) on its surface. The presence of local inhomogeneities, chemical composition and surface morphology in thin film are directly related to the surface water contact angle. Both super-hydrophilic and super-hydrophobic surfaces are important for practical applications. The wettability behavior is characterized by the value of contact angle, a macroscopic parameter [20]. In the present case, the water lies with contact angle of 14° on the surface of PPy film in between porous spherical bunches of nanoplates as seen in Fig. 6, indicating that PPy is an intrinsically hydrophilic material. The nanoplate like surface morphology of the PPy might have caused for lower water contact angle value. This specific property is attributed to the nanocrystalline nature that is expected to possess very high surface energy [21].

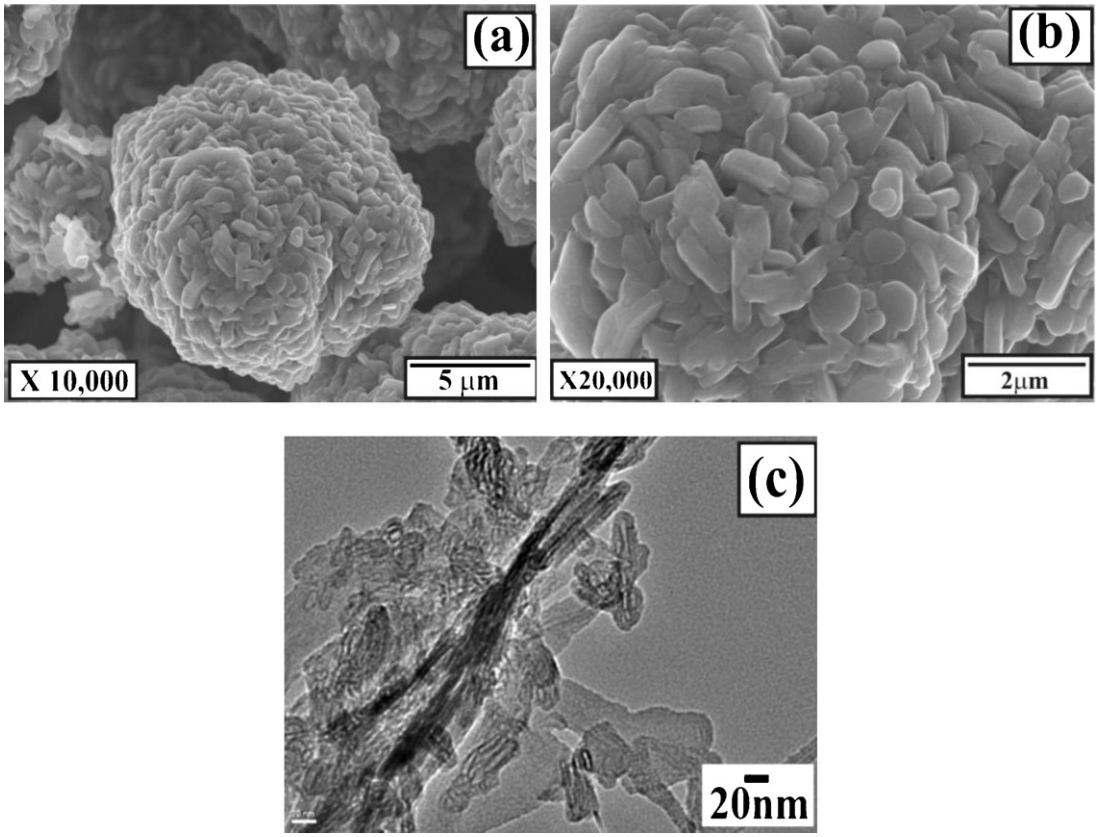

Fig. 5. Scanning electron micrographs of PPy thin films at two different magnifications (a) ×10,000, (b) ×20,000 and (c) TEM image of PPy thin film.

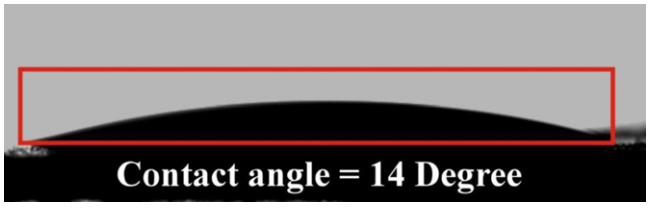

Fig. 6. Measurement of water contact angles for PPy thin films.

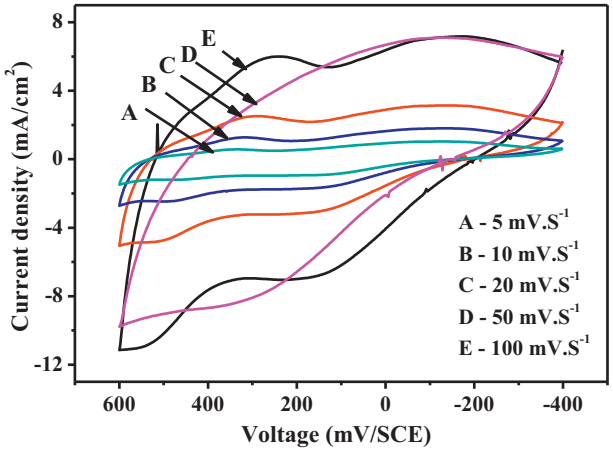

Fig. 7. Cyclic voltammograms of PPy thin films at different scanning rates (A – 5 mV s^{-1}, B – 10 mV s^{-1}, C – 20 mV s^{-1}, D – 50 mV s^{-1}, E – 100 mV s^{-1}) in 0.5 M H_2SO_4 electrolyte.

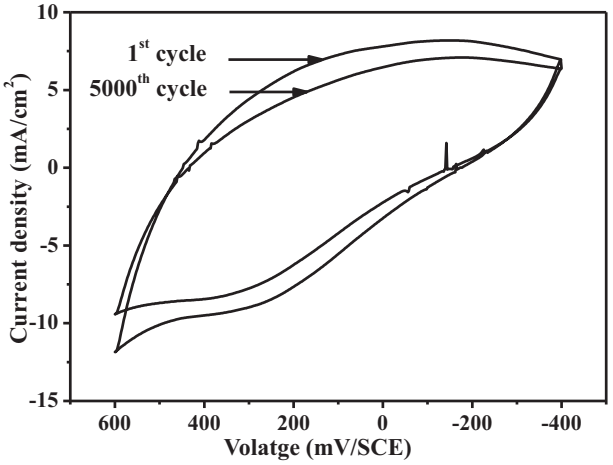

Fig. 8. Cyclic voltammograms of PPy thin films at different number of cycles at 100 mV s^{-1} in 0.5 M H_2SO_4 electrolyte.

3.6. Electrochemical studies

3.6.1. Scan rate variation

To estimate the electrochemical behavior of the PPy electrode, Fig. 7 gives cyclic voltammetric curves for PPy nanoplates in the potential of −0.4 to 0.6 V/SCE at scan rates of 5, 10, 20, 50 and 100 mV s^{-1}. Compared with the curves at different scan rates, all the curves displayed two pairs of oxidation and reduction peaks, which indicated that the current–potential response was potential dependent and the pseudocapacitance mainly derived from the

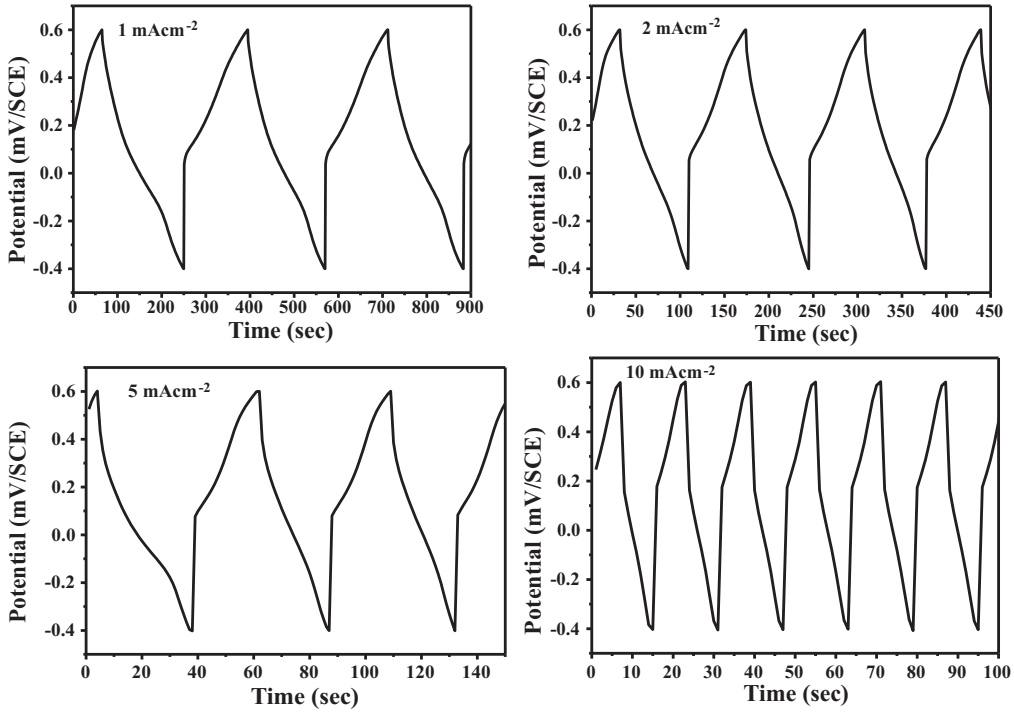

Fig. 9. Galvanostatic charge–discharge curves of PPy thin films at different current densities (1, 2, 5 and 10 mA cm^{-2}).

redox reaction of PPy electrode. Nanoplates of PPy electrode shows the capacitive-like responses in the whole potential range of investigation at different scan rates of CV in Fig. 7 along with the current under the curve increases slowly with the scan rate. The maximum specific capacitance of 533 F g^{-1} at the scan rate of 5 mV s^{-1} was obtained. The specific and interfacial capacitance values decreases from 533 to 412 F g^{-1} and 0.034 to 0.019 F cm^{-2}, respectively. The decrease in capacitance has been attributed to the presence of inner active sites that cannot sustain the redox transitions completely at higher scan rates. This is probably due to the diffusion effect of protons within the electrode. The decreasing trend of the capacitance suggests that parts of the surface of the electrode are inaccessible at high charging–discharging rates.

3.6.2. Stability study

The cyclic stability of the nanoplates of PPy electrode at the sweep rate of 100 mV s^{-1} for 1st and 5000th cycles are shown in Fig. 8. From the figure it is seen that specific capacitance of PPy electrode decreased from 533 to 408 F g^{-1} in the 5000 cycles. This demonstrates that the material is suitable for energy-storage applications. The specific and interfacial capacitance values are decreased by a small amount with the number of cycles due to the loss of active material caused by the dissolution and/or detachment, during the early charging/discharging cycles in the electrolyte. The 78% cyclic stability of the nanoplates of PPy electrode was observed.

3.6.3. Galvanostatic charge–discharge measurement

Galvanostatic charge/discharge, at various current densities of 1, 2, 5 and 10 mAcm^{-2}, was performed in order to better understand the behavior of the obtained PPy for supercapacitor applications. Typical galvanostatic charge/discharge curves of PPy electrode is presented in Fig. 9. It could be seen that all the curves were not ideal straight line, indicating the process of a faradic reaction. In addition, there was an initial drop in potential caused by internal resistance. With the decrease of the charge/discharge current density, this potential drop became less. The specific capacitance (Cs) can be calculated as follows:

$$Cs = \frac{I \times \Delta t}{\Delta V \times m} \quad (3)$$

where Cs is specific capacitance, I is charge/discharge current, Δt is the discharge time, ΔV is 1 V, and m is the mass of active material within the electrode. It was clear that the PPy nanoplates had a good electrochemical reversibility and a large specific capacitance (528 F g^{-1}). The value of specific capacitance obtained by charge–discharge and CV technique are comparable.

4. Conclusions

Novel and simple two step chemical method has been developed for the fabrication of 3D nanostructure of PPy electrode. The presence of characteristics bonds of PPy were confirmed from FTIR studies. The SEM study revealed that PPy films have 3D spherical bunches of interconnected nanoplates. Polypyrrole electrode showed maximum specific capacitance of 533 F g^{-1} at 5 mV s^{-1}. Thus, these PPy electrodes can open new opportunities in a myriad of applications, such as energy storage systems, catalysis, fuel cell membranes, nanoelectronics devices, and antibacterial coatings. The method is general and can be extended to other conducting polymers, such as polythiophene and polyaniline.

Acknowledgments

Authors are grateful to the Council for Scientific and Industrial Research (CSIR), New Delhi (India) for financial support through the scheme No. 03(1165)/10/EMR-II. One of the authors Prof. C.D. Lokhande is also grateful to All India Council for Technical Education (AICTE), New Delhi for financial support through the scheme F. No. 8023/BOR/RID/RPS-165/2009-10.

References

[1] C.M. Yang, Y.J. Kim, M. Endo, H. Kanoh, M. Yudasaka, S. Iijima, K. Kaneko, J. Am. Chem. Soc. 129 (2007) 20.
[2] C.C. Hu, Y.H. Huang, K.H. Chang, J. Power Sources 108 (2002) 117.
[3] Z. Mandic, M.K. Rokovic, T. Pokupcic, Electrochim. Acta 54 (2009) 2941.
[4] Q. Wu Zhang, X. Zhou, H.-S. Yang, J. Power Sources 125 (2004) 141.
[5] H.C. Kang, K.E. Geckeler, Polymer 41 (2000) 6931.
[6] K. Hycok, A.K. Ku, J. Jeong, J. Electrochem. Soc. 149 (2002) A1058.
[7] R.K. Sharma, A.C. Rastogi, S.B. Desu, Electrochem. Commun. 10 (2008) 268.
[8] C. Weidlich, K.M. Mangold, K. Juttner, Electrochim. Acta 50 (2005) 1547.
[9] Y.L. Xu, J. Wang, W. Sun, S.H. Wang, J. Power Sources 159 (2006) 370.
[10] C. Yang, P. Liu, Y. Zhao, Electrochim. Acta (2010), online available.
[11] H. An, Y. Wang, X. Wang, L. Zheng, X. Wang, L. Yi, L. Bai, X. Zhang, J. Power Sources 195 (2010) 6964.
[12] C. Shi, I. Zhitomirsky, Nanoscale Res. Lett. 5 (2010) 518.
[13] R. Ansari, J. Chem. 3 (2006) 186.
[14] K.L. Chopra, Thin Film Phenomena, McGraw Hill Book Co, New York, 1969.
[15] S.P. Palaniappan, P. Manisankar, Mater. Chem. Phys. 122 (2010) 15.
[16] C. Yang, T. Wang, P. Liu, H. Shi, D. Xue, Solid State Mater. Sci. 13 (2009) 112.
[17] X. Yang, L. Li, Synthetic Metals 160 (2010) 1365.
[18] A.J.F. Romero, J.J.L. Cascales, T.F. Otero, J. Phys. Chem. B 109 (2005) 21078.
[19] S.T. Selvan, Chem. Commun. 3 (1998) 351.
[20] D.S. Dhawale, R.R. Salunkhe, V.S. Jamadade, D.P. Dubal, S.M. Pawar, C.D. Lokhande, Curr. Appl. Phys. 10 (2010) 904.
[21] K.K.S. Lau, J. Bico, K.B.K. Teo, M. Chhowalla, G.A.J. Amaratunga, W.I. Milne, G.H. McKinley, K.K. Gleason, Nano Lett. 3 (2003) 1701.